

physics department

from nanomaterials to new sensor applications

António Luís Ferreira – alf@ua.pt





research areas

materials physics/ nanosciences and nanotechnology

photovoltaic materials

optics and photonics

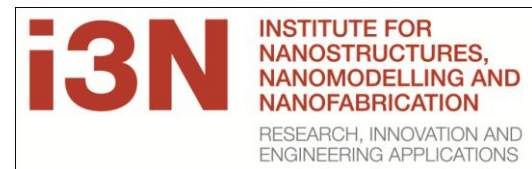
biophysics and medical physics

radiation detectors

complex system physics and physics of networks

astronomy and astrophysics

meteorology, climatology and oceanography



university of aveiro
theoria poiesis praxis



ciceco
centre for research in ceramics & composite materials

research labs and research units

i3n, ciceco, cesam, cidtff



CESAM
Centre for Environmental and Marine Studies
www.cesam.ua.pt



people

- › teaching staff: 48.6
- › non-teaching staff: 14 (+1 I3N)
- › researchers: 15
- › postdocs: 25
- › phd students: ~ 50

research output

› papers : ~ 150 per year

research funding (2010)

- › knowledge valorization 193 k€
- › public national 2 052 k€
- › EU 316 k€
- Total 2 561 k€

› citations per paper 2005/10 : 5.8



astronomy and astrophysics

› People

Alexandre Correia, Helena Morais, Cristian Giuponne

› studies of evolution of planet rotation

› paleoclimatology of earth and mars

› search for extra-solar planets, stellar wobble

› tidal and core-mantle friction effects

› some references

Correia and Laskar, Nature 429(6994): 848-850 (2004)

Lovis, C., et al. Nature 441(7091):305-09(2006)

Correia, Laskar, et.al. Celestial Mechanics & Dynamical Astronomy 111, no. 1-2 (Oct 2011): 105-30.

Morais, M. H., and Correia Astronomy & Astrophysics 525 (Jan 2011).

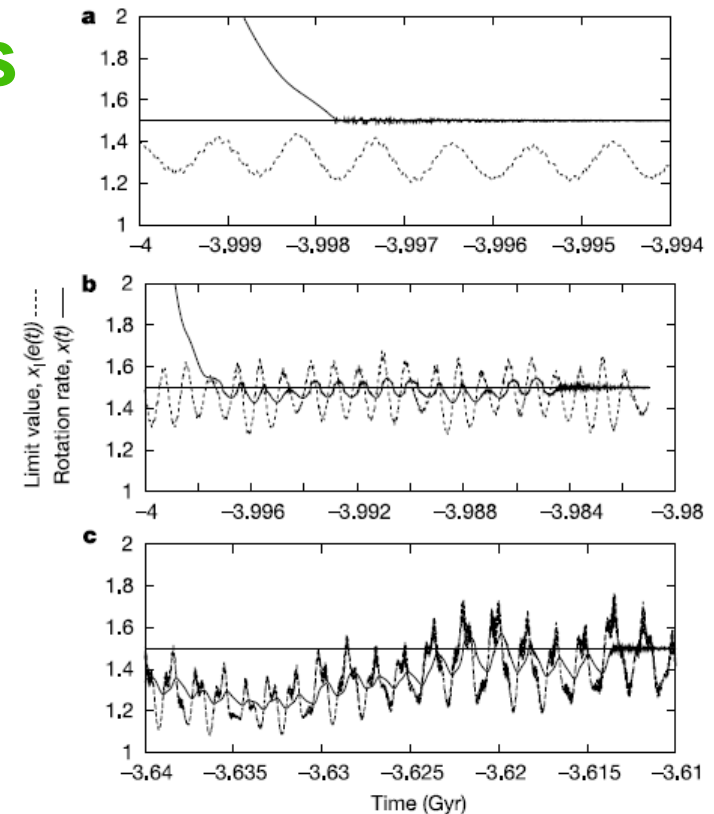


Figure 2 Typical cases of capture into the 3/2 resonance. The rotation rate $x(t)$ (bold curve) and limit value $x_l(e(t))$ (dotted curve) are plotted versus time (Gyr). **a**, Type I is the classical case⁵: As $e < e_{3/2}$, the limit value x_l is always lower than 3/2. **b**, In Type II, at the time when x reaches the resonant value 3/2, e is oscillating around $e_{3/2}$, leading to multiple crossings of the resonance, with ultimately a capture. **c**, Type III corresponds to solutions that have not been captured during the initial crossing of the resonance, but later on, as the eccentricity increases beyond $e_{3/2}$.

gravitation

› People

Carlos Herdeiro, Marco Sampaio, Carmen Rebelo

› numerical relativity for D dimensional space-times

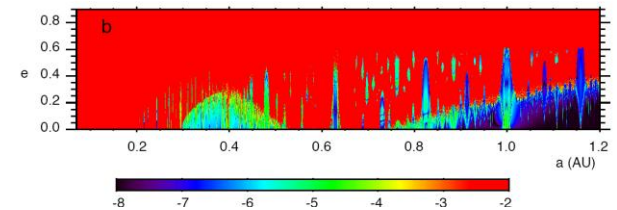
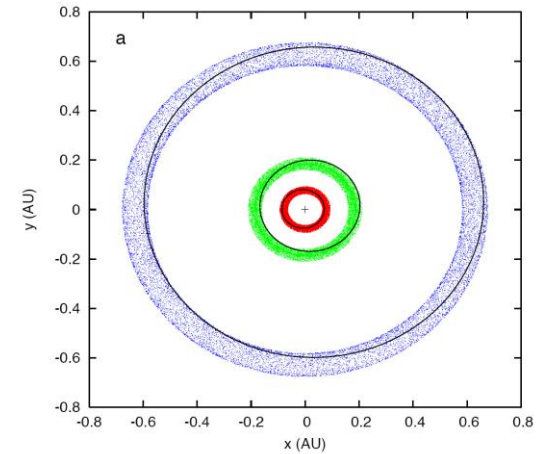
› collisions of black holes

› some references

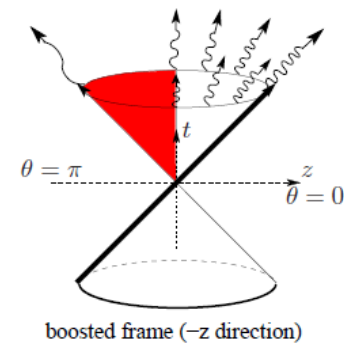
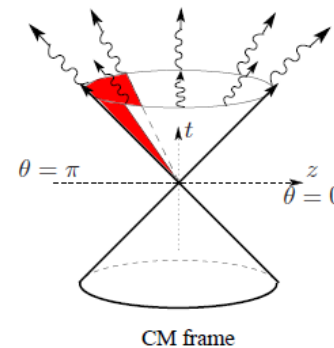
Witek, H., et. al, Phys. Rev. D 83, 044017 (2011).

Herdeiro, C, Sampaio M, and Rebelo C, J. High Energy Physics, 7 (2011).

Avelino, P., et al. Physical Review D 84(2) (2011)



An extrasolar planetary system with three Neptune-mass planets



MagLab

Materials research for magnetic sensors

› People

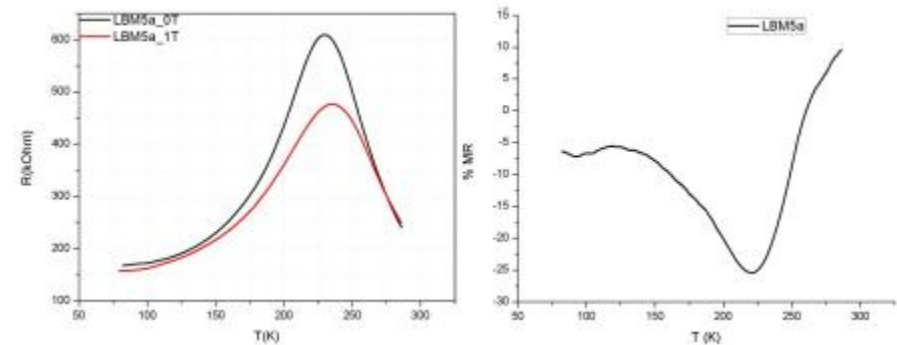
Vítor Amaral, Armando Lourenço, Nuno Silva,
João Amaral, Das Soma.
Fábio Figueiras, João Gonçalves

› magnetoresistance

› applications of magnetic fied sensors:

magnetic data storage in hard disks
strain measurement and actuators

Metal or oxide materials, in thin film, heterostructures
and tunnel junctions are used, the choice depending on
conditions



Example of temperature dependence of electric resistivity and magnetoresistance (at field 1 Tesla) of manganite thin film La-Ba MnO₃

on-going work :

Magnetic Shape Memory alloy/Piezoelectric heterostructures

Ferromagnetic manganite oxide thin films for magnetoresistance

Ferromagnetic/ferroelectric multiferroic oxide heterostructures

MagLab

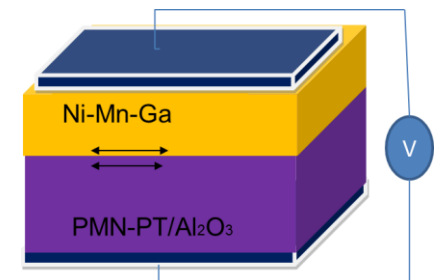
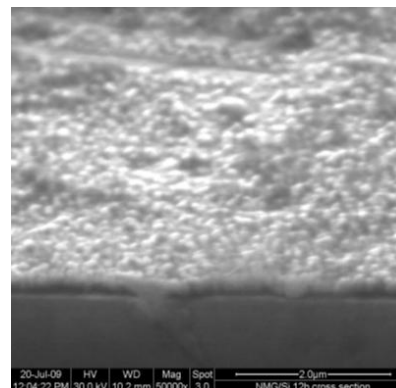
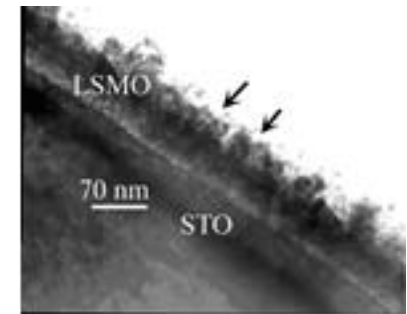
› **New approaches:** coupled ferroelectricity/ferroelasticity in multiferroic devices have been proposed. This opens also the possibility for combined electric field polarization.

› **studies and develops:** (epitaxial or polycrystalline) thin films and structures by magnetron sputtering that can be used/optimized for magnetic sensing/actuating in varied temperature ranges (10-320K)

Example of heterostructure:
Scanning Electron microscope image of magnetic shape memory alloy film on silicon

Scheme of multiferroic structure with piezoelectric/oxide

Transmission Electron microscope image of manganite thin film on oxide substrate



Wide band gap semiconductor oxides for optoelectronics and gas sensing applications

› People

T. Monteiro, A. Neves, J. Soares, R. Correia, J. Leitão, N Sobolev, F. Costa, A. Cunha, Marco Peres, L. C. Costa, etc

› wide band gap oxides

› semiconducting devices for gas detection.

gas adsorption onto a semiconductor produces a conductance change

ZnO – n type semiconductor

□ Materials

□ ZnO, MgO, SnO₂, TiO₂, Fe₂O₃, Al₂O₃, SrTiO₃, LiNbO₃, Ta₂O₅, CCTO, and alloys

□ ZnS, ZnSe, CdS, CdSe

□ GaN, InGaN, AlGaN, AlN
AlInGaN

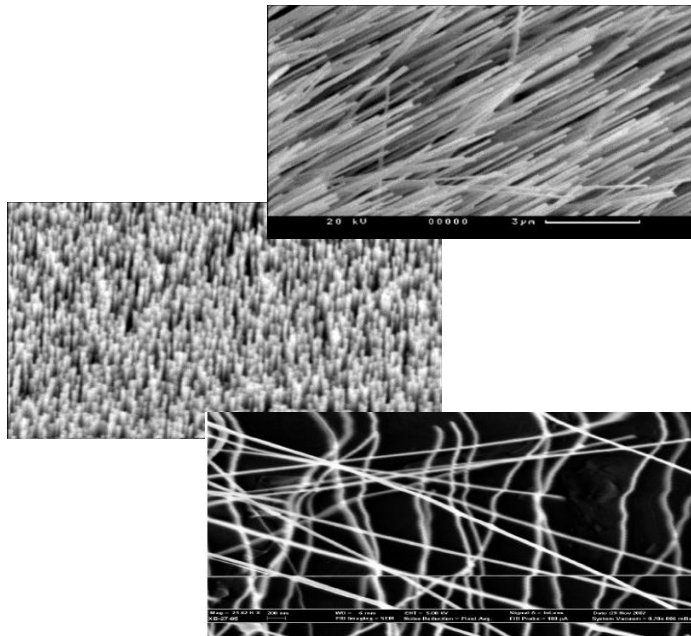
□ porous-Si, Si/Ge, nc-Si,
InAs/InP

□ nc-diamond, SWCT, MWCT

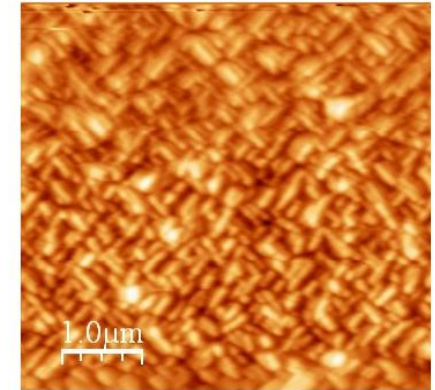
□ nano metal-organic
complexes

Wide band gap semiconductor oxides for optoelectronics and gas sensing applications

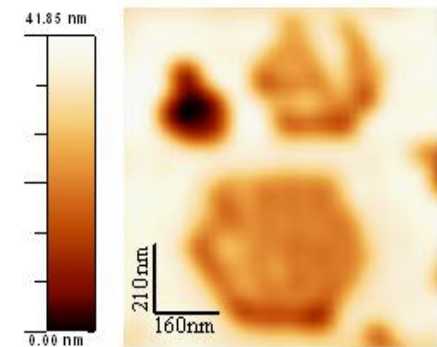
› Oxygen-related gas sensing chemisorption of oxygen on oxide surface, followed by charge transfer during the reaction between the chemisorbed oxygen and target gas molecules, change the surface resistance



ZnO
films
heterojunctions
nanoparticles
nanowires



A. S. Lourenço, et al., (2008)



M. Peres, et al., (2008)

Wide band gap semiconductor oxides for optoelectronics and gas sensing applications

› Issues:

- Sensitivity
- Gas Selectivity
- Reproducibility
- Rapid response time
- Adequate operating temperature

- Avoid long term instability and sensitivity to ambient humidity
- Adding of catalysts

device resistivity changes with changes in CO concentration

ZnO nanowire based CO detector, S. Chang et al.,
Nanotechnology 19 (2008) 175502

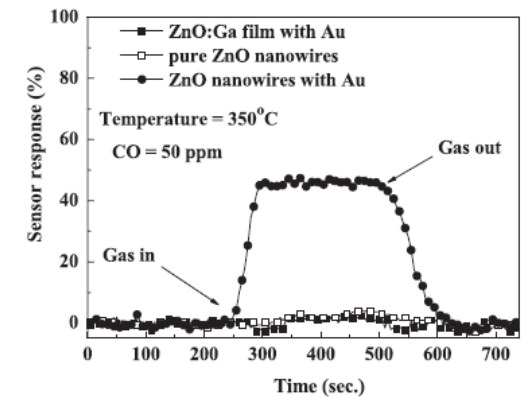


Figure 4. Detector responses of the ZnO nanowire-based CO gas sensors measured at 350 °C. Sensor response of the sample with only the patterned ZnO:Ga film and Au adsorption was also plotted.

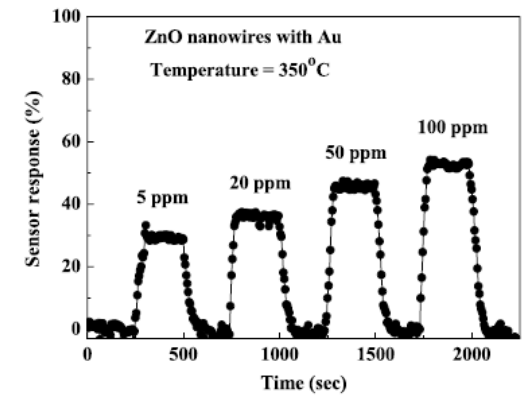


Figure 5. Response of the ZnO nanowire CO gas sensor measured with various CO concentrations.



Materials
Views

www.MaterialsViews.com

Adv. Mater. 2010, 22, 4499–4504

ADVANCED
MATERIALS

www.advmat.de

A Luminescent Molecular Thermometer for Long-Term Absolute Temperature Measurements at the Nanoscale

By Carlos D. S. Brites, Patricia P. Lima, Nuno J. O. Silva, Angel Millán, Vitor S. Amaral, Fernando Palacio,* and Luís D. Carlos*

Thermometry at nanoscale

› People

Luís Carlos, Patrícia Lima

Rute André, Carlos Brites, Vitor

Amaral, Nuno Silva

› Luminescent non-contact thermometers

Optical probes (organic dyes or trivalent lanthanides, Ln³⁺) emitting visible light (thermochromic materials)

Advantages

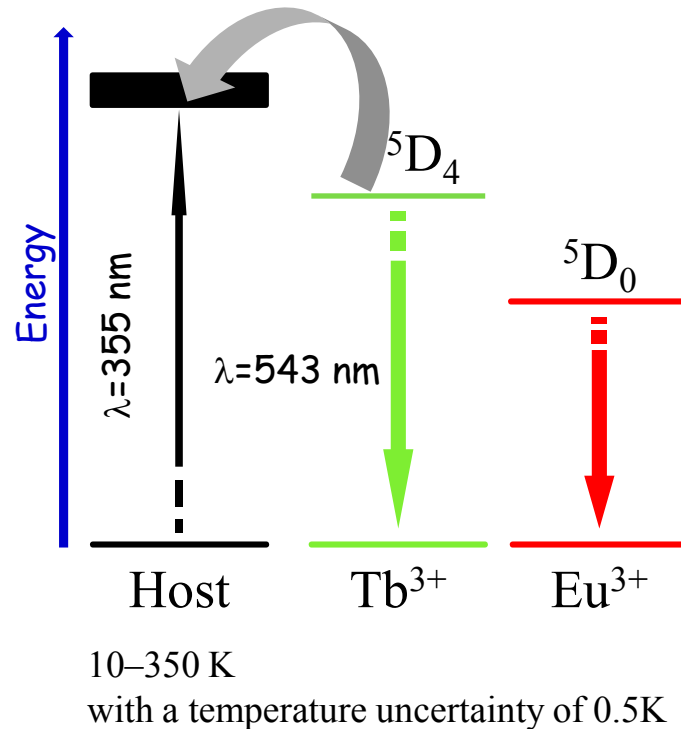
- › Noninvasive and accurate technique that works remotely by way of an optical detection system, even in biological fluids, strong electromagnetic fields and fast-moving objects
- › Intensity ratio of two emissions provide self-calibration

Disadvantages

- › Some examples use complex analysis of lifetimes or emission quantum yields
- › Intensity decreases drastically under continuous excitation (photobleaching): not suitable for long-term monitoring (organic dyes)

Eu/Tb luminescent nanothermometer

The breakthrough...



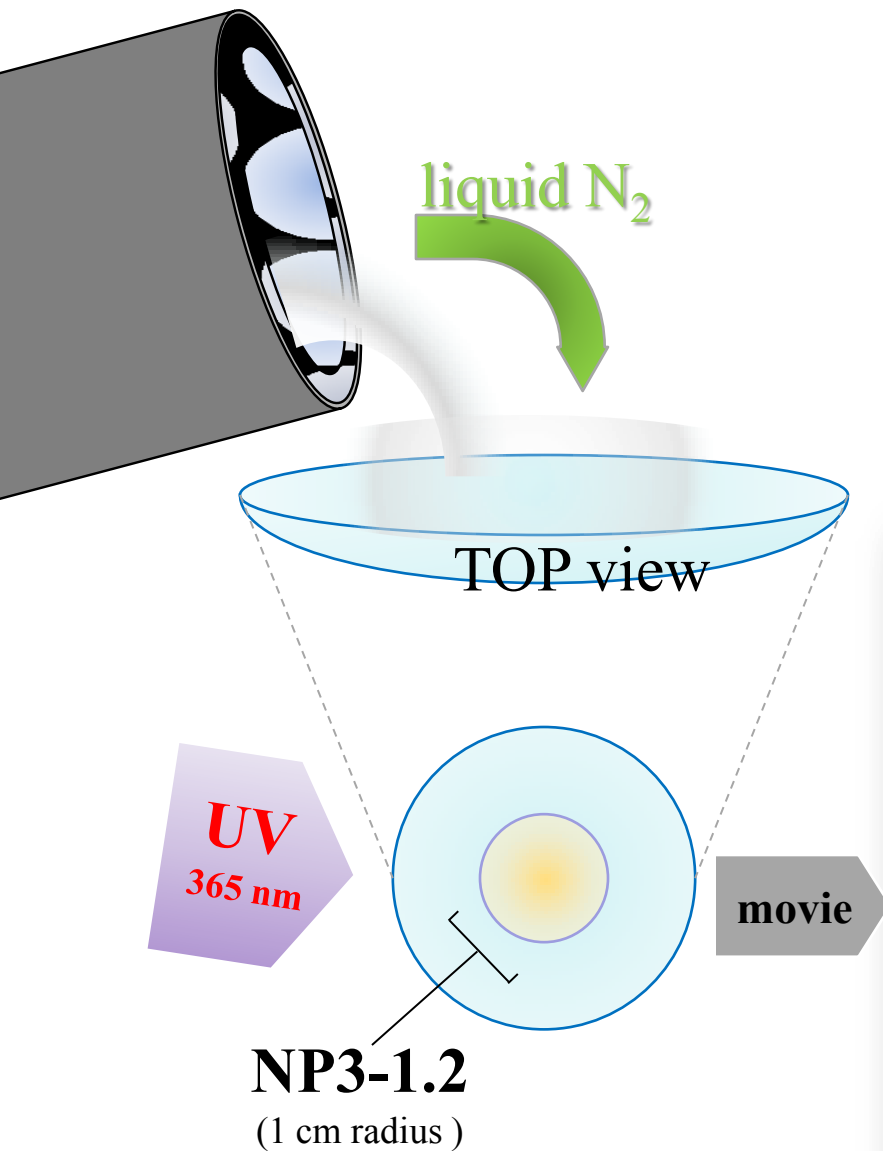
› **Host rational design**; an excited triplet with energy above that of the $Tb^{3+} {}^5D_4$ state, thus warranting the occurrence of thermally-driven ${}^5D_4 \rightarrow$ host energy transfer

› ΔE between that triplet state and the $Eu^{3+} {}^5D_0$ emitting level is too large to permit thermally-driven depopulation

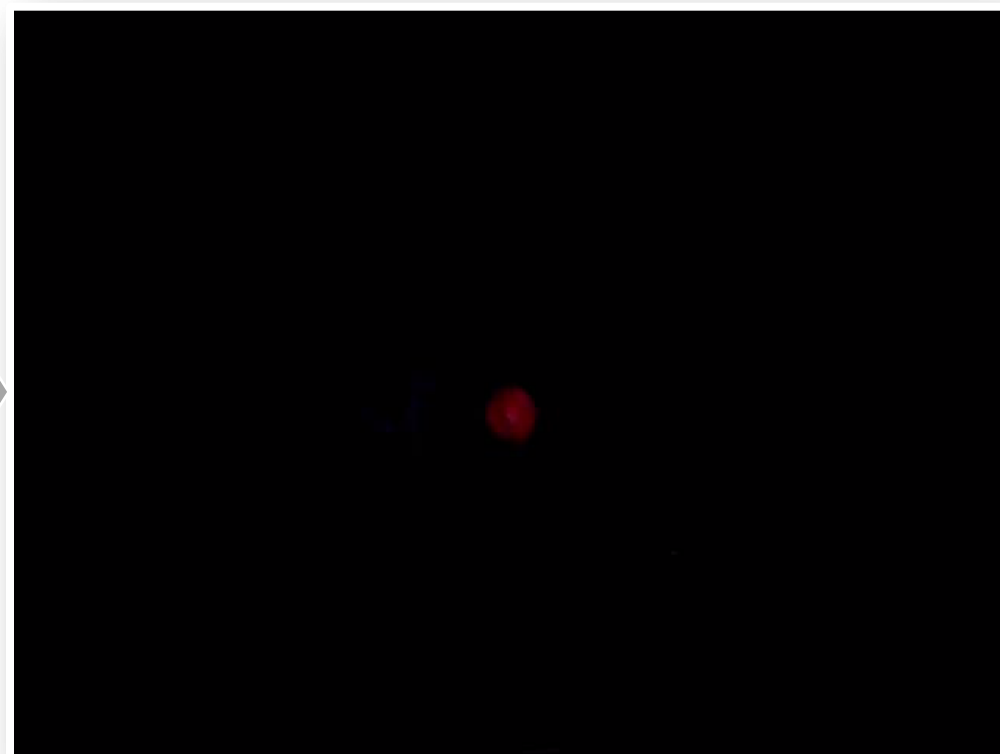
› The Tb/Eu relative intensity guarantees **absolute measurement of temperature**

› **The self-calibration** (relative intensities) overcomes the well-known drawbacks of intensity-based measurements (*e.g.* sensor concentration)

Spain Patent P200930367, 2009; **Adv. Mater.**, 2010, 22, 4499; **New J. Chem.**, 2011, 35, 1177



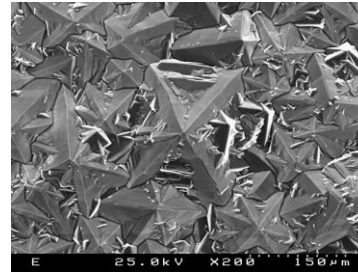
NP3-1.2 : color/temperature dependence



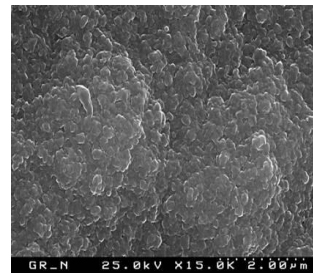
Micro-wave plasma chemical vapor deposition diamond MPCVD

› People

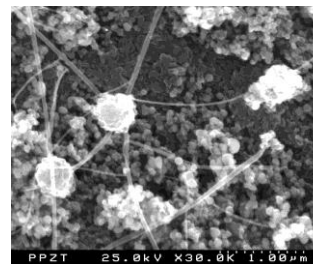
Florinda Costa, A. J. Fernandes,



Microcrystalline
diamond



Nanocrystalline
diamond



Composite of
nanocrystalline
diamond and carbon
nanotubes

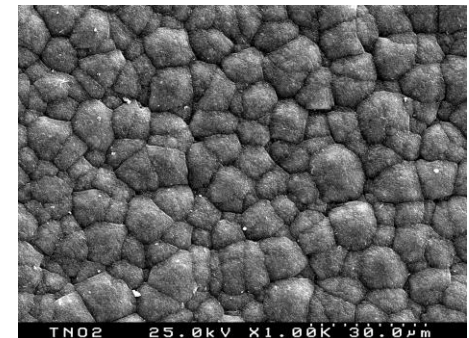
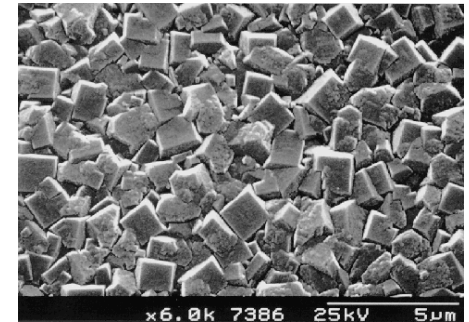
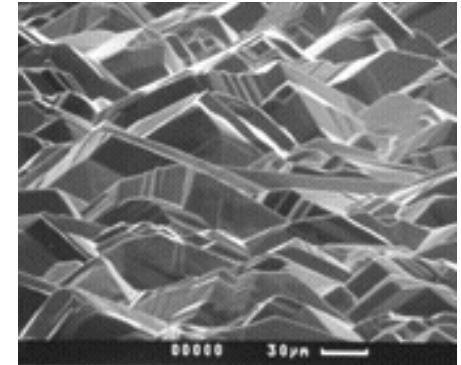
CVD diamond applications

electronic devices: particle detectors for high energy, high power diodes, cold cathode and SAW filters (surface acoustic wave)

optical applications: optical transparency in a wide range in the electromagnetic spectrum, windows microwave and X-rays, screens and leds

sensors: detectors of radiation in a broad spectrum, optical fiber communications, detectors of nuclear radiation

Dosimetry applications: dosimeters in radiotherapy, active exposure monitoring



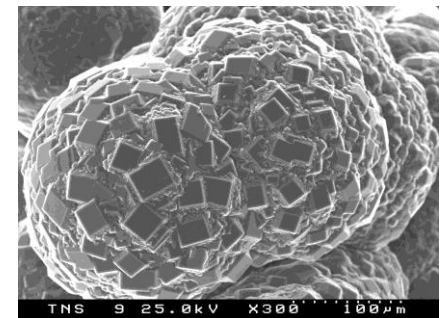
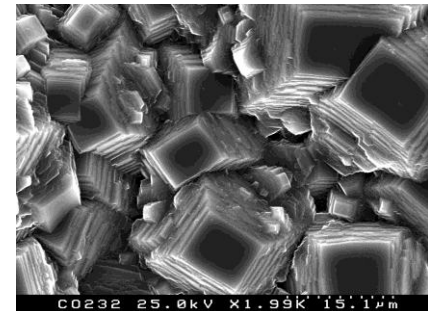
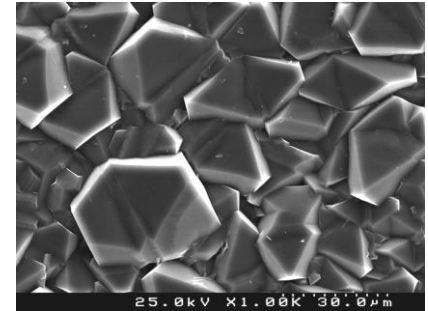
CVD diamond applications

acoustic applications: ultrasonic detectors for medical diagnostics and nondestructive quality control in the industry

hardware components: the high wear resistance opens the possibility of the hard disks and optical disks are coated with diamond.

applications in biomedicine: Due to the high chemical inertness and biocompatibility is used in implants and prostheses, combining the high wear resistance is used as surgical tools, orthopedic and dental drills

Nuclear applications: homeland security, nuclear reactors and fusion experiments



applications NcD and NT

Microelectronics

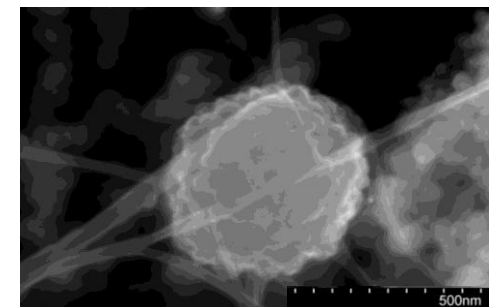
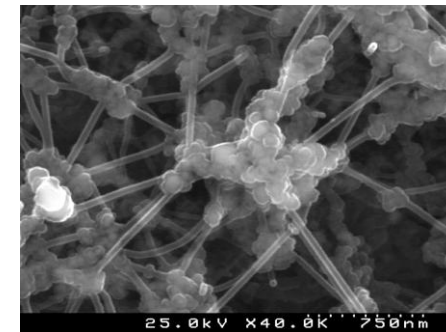
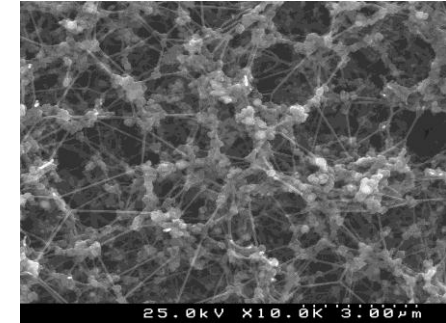
field emission devices, field shielding in
MEMS/NEMS (Micro/Nano-Electro-Mechanical
Systems)

Electrochemistry

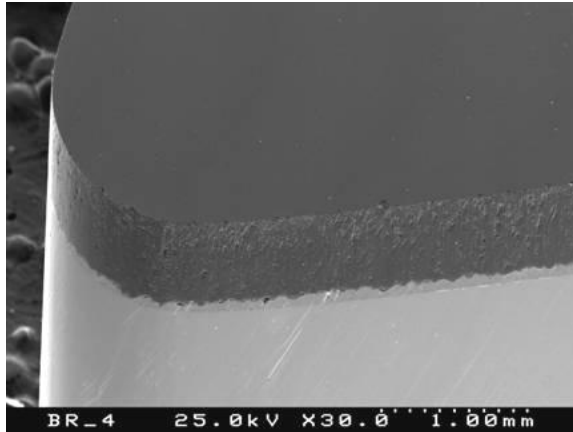
electrodes in supercapacitors, biomolecule
sensors

Electronics

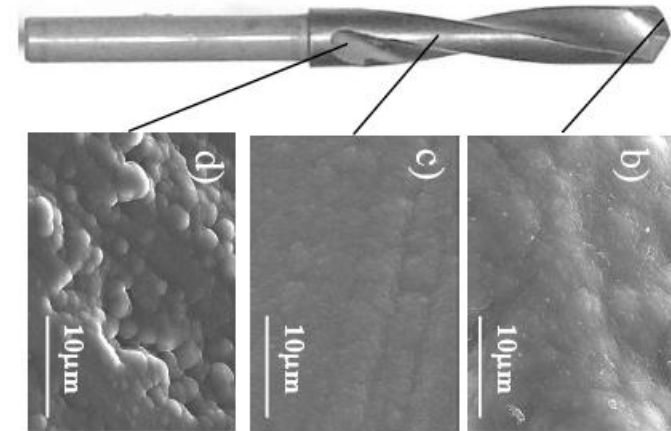
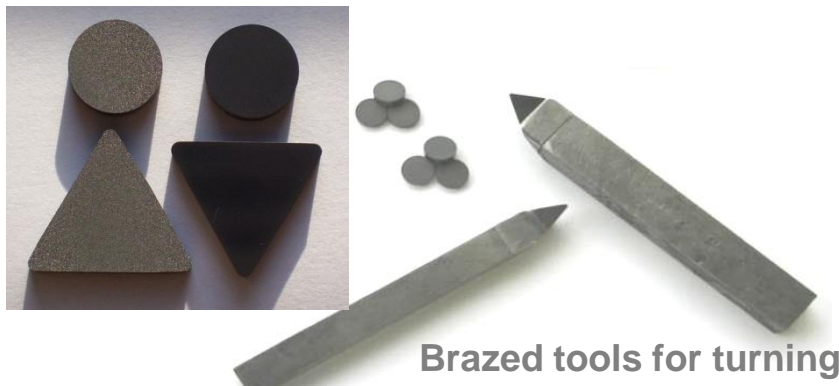
thermal management of ICs, thermionic
energy generation



Cutting tools for non-ferrous abrasive materials: indexable inserts for turning and milling, drilling and milling machine



Coated ceramic tools



Details of the nanodiamond coating
on Si₃N₄ drill

